



**HAL**  
open science

## Geological evidence of extensive N-fixation by volcanic lightning during very large explosive eruptions

Adeline Aroskay, Erwan Martin, Slimane Bekki, Jean-Luc Le Penneec, Joël Savarino, Abidin Temel, Nelida Manrique, Rigoberto Aguilar, Marco Rivera, Herve Guillou, et al.

### ► To cite this version:

Adeline Aroskay, Erwan Martin, Slimane Bekki, Jean-Luc Le Penneec, Joël Savarino, et al.. Geological evidence of extensive N-fixation by volcanic lightning during very large explosive eruptions. Proceedings of the National Academy of Sciences of the United States of America, 2024, 121 (7), pp.e2309131121. 10.1073/pnas.2309131121 . hal-04446185

**HAL Id: hal-04446185**

**<https://hal.science/hal-04446185>**

Submitted on 11 Jul 2024

**HAL** is a multi-disciplinary open access archive for the deposit and dissemination of scientific research documents, whether they are published or not. The documents may come from teaching and research institutions in France or abroad, or from public or private research centers.

L'archive ouverte pluridisciplinaire **HAL**, est destinée au dépôt et à la diffusion de documents scientifiques de niveau recherche, publiés ou non, émanant des établissements d'enseignement et de recherche français ou étrangers, des laboratoires publics ou privés.

1

2

## 3 **Revised Main Manuscript for**

## 4 Geological evidence of extensive N-fixation by volcanic lightning 5 during very large explosive eruptions

6

7 Adeline Aroskay<sup>1\*</sup>, Erwan Martin<sup>1\*</sup>, Slimane Bekki<sup>2</sup>, Jean-Luc Le Pennec<sup>3</sup>, Joël Savarino<sup>4</sup>, Abidin  
8 Temel<sup>5</sup>, Nelida Manrique<sup>6</sup>, Rigoberto Aguilar<sup>6</sup>, Marco Rivera<sup>7</sup>, Hervé Guillou<sup>8</sup>, Hélène Balcone-  
9 Boissard<sup>1</sup>, Océane Phelip<sup>1</sup>, Sophie Szopa<sup>8</sup>

10

11 1: Institut des Sciences de la Terre de Paris (ISTeP), Sorbonne Université ; Paris, France.

12 2: Laboratoire Atmosphères, Observations Spatiales (LATMOS), SU/UVSQ ; France.

13 3: Institut de Recherche pour le Développement (IRD) & Institut Universitaire Européen de la  
14 Mer ; Plouzané, France.

15 4: Institut des Géosciences de l'Environnement (IGE) ; Grenoble, France.

16 5: Hacettepe University, Department of Geological Engineering; Ankara, Turkey.

17 6: Instituto Geológico Minero y Metalúrgico (INGEMMET), Observatorio Vulcanológico del  
18 INGEMMET; Arequipa, Peru.

19 7: Instituto Geofísico del Perú, Observatorio Vulcanológico del Sur ; Arequipa, Peru.

20 8: Laboratoire des Sciences du Climat et de l'Environnement (LSCE), Université Paris-Saclay ;  
21 France.

22 \*Corresponding authors. Email: [adeline.aroskay@sorbonne-universite.fr](mailto:adeline.aroskay@sorbonne-universite.fr),  
23 [erwan.martin@sorbonne-universite.fr](mailto:erwan.martin@sorbonne-universite.fr)

24

### 25 **Author Contributions:**

26 Conceptualization: AA, EM, SB, SS

27 Sampling: AA, EM, SS, JLL, JLLP, AT, NM, RA, MR, HG, HBB

28 Analyses: AA, OP

29 Writing: AA, EM, SB, SS, JLLP, JS

30 **Competing Interest Statement:** All the Authors declare that they have no competing interests

31 **Classification:** Physical sciences / Earth, atmospheric and planetary sciences

32 **Keywords:** volcanic lightning, oxygen multi-isotopes, nitrate

33

34 **This PDF file includes:**

35 Main Text

36 Figures 1 to 4

37

38 **Abstract**

39 Most of the nitrogen (N) accessible for life is trapped in dinitrogen (N<sub>2</sub>), the most stable  
40 atmospheric molecule. In order to be metabolized by living organisms, N<sub>2</sub> has to be converted  
41 into biologically assimilable forms, so-called fixed N. Nowadays, nearly all the N-fixation is  
42 achieved through biological and anthropogenic processes. However, in early prebiotic  
43 environments of the Earth, N-fixation must have occurred via natural abiotic processes. One of  
44 the most invoked processes is electrical discharges, including from thunderstorms and lightning  
45 associated with volcanic eruptions. Despite the frequent occurrence of volcanic lightning during  
46 explosive eruptions and convincing laboratory experimentation, no evidence of substantial N-  
47 fixation has been found in any geological archive. Here we report on the discovery of significant  
48 amount of nitrate in volcanic deposits from Neogene caldera-forming eruptions, which are well  
49 correlated with the concentrations of species directly emitted by volcanoes (sulphur, chlorine).  
50 The multi-isotopic composition ( $\delta^{18}\text{O}$ ,  $\Delta^{17}\text{O}$ ) of the nitrates reveals that they originate from the  
51 atmospheric oxidation of nitrogen oxides formed by volcanic lightning. According to these first  
52 geological volcanic nitrate archive, we estimate that, on average, about 60 Tg of N can be fixed  
53 during a large explosive event. Our findings hint at a unique role potentially played by subaerial  
54 explosive eruptions in supplying essential ingredients for the emergence of life on Earth.

55

56 **Significance Statement**

57 Nitrogen (N) fixation is an essential process for life as it converts atmospheric dinitrogen into  
58 biologically assimilable forms. Experimental and theoretical studies have proposed that volcanic  
59 lightning could have contributed to N-fixation in early prebiotic environments on Earth but  
60 geological evidence are still lacking. For the first time, significant amounts of nitrate, the oxidation  
61 end product of atmospheric N-fixation, have been discovered in volcanic deposits from very large

62 explosive eruptions. Geochemical analysis, including oxygen multi-isotopes, indicates that the  
63 origin of this nitrate is N-fixation by volcanic lightning. These findings provide geological support  
64 for a unique role played by subaerial explosive eruptions in high energy-demanding processes,  
65 which were essential in supplying building blocks for life during its emergence on Earth.

66

67

## 68 **Introduction**

69

70 Nitrogen (N) is an essential element for life and its main atmospheric form today is dinitrogen  
71 ( $N_2$ ), the most stable atmospheric molecule. In order to be metabolised by living organisms,  $N_2$   
72 has to be converted into biologically assimilable forms, so-called fixed N. Nowadays, N-fixation is  
73 dominantly achieved through biological and anthropogenic processes (1). In early prebiotic  
74 environments on Earth, N-fixation, which supported the emergence of life, must have occurred  
75 only via natural abiotic processes. Several hypotheses have been proposed including  
76 photochemical reactions, hydrothermal reduction, lightning discharges, thermal reduction over  
77 magma, and meteoric impact-induced shocks (2–4). So far, the lack of identified geological  
78 archives of fixed N corroborating the existence of such processes has prevented the confirmation  
79 and quantification of these possible abiotic mechanisms on Earth. One of the most invoked  
80 processes is lightning from thunderstorms but also lightning associated with volcanic eruptions  
81 (3). Due to the electrification of the ash- and water-rich volcanic plumes, volcanic lightning (VL)  
82 occurs systematically during explosive eruptions (5). Lightning strokes detection in volcanic  
83 regions also serves nowadays as a potential eruption alert indicator (6, 7). Experimental  
84 laboratory studies and thermodynamic models suggest that VL can contribute significantly to N-  
85 fixation over the Earth history (8, 9). However, no geological evidence of substantial N-fixation by  
86 VL has ever been found so far. We report here the discovery in volcanic deposits of significant  
87 amount of nitrate, which multi-oxygen and nitrogen isotopes composition points toward  
88 atmospheric N-fixation induced by VL.

89 In search for volcanic fixed N, we targeted nitrates ( $NO_3^-$ ), the nitrogen oxidation end-  
90 product, in volcanic deposits from very large eruptions (for which VL is expected to be extensive)  
91 in arid to semi-arid environments, which are most favourable to the preservation of deposit  
92 integrity. We considered volcanic deposits from Neogene caldera-forming eruptions (1.6 to 20  
93 Ma; volcanic explosivity index VEI of about 7), in Turkey (Anatolia) and Peru (North of the Andean  
94 Central Volcanic Zone) (10, 11). Samples were collected from volcanic tephra fallout deposits and  
95 large-volume pyroclastic density current (PDC) deposits called ignimbrites. For comparison, 3  
96 samples were also collected in a non-arid environment and more recent tephra fallout deposits

97 of 2 large explosive eruptions from Ischia, Italy (the Tischiello eruption: ~75kyrs; VEI of about 3-4  
98 and the Monte Epemeo Green Tuff eruption – MEGT: ~55kyrs; VEI of about 5-6; (12)). Indeed,  
99 atmospheric (non-volcanic) nitrate deposition and accumulation overtime in volcanic deposits  
100 could at first be considered possible (13). Such mechanism could contribute significantly to the  
101 nitrate budget of volcanic samples in an arid-environment (for the sake of nitrate conservation  
102 overtime) and over long period of time (few Myrs typically). Therefore, the contribution of long  
103 term atmospheric nitrate deposition and accumulation overtime is unlikely to be efficient for young  
104 volcanic deposits (about tens of kyrs old) in a non-arid environment like Ischia.

105

106

## 107 **Results and discussion**

108

109 ***Nitrate from volcanic deposits are linked to the explosive eruption event:*** The most  
110 remarkable finding is the unexpectedly high  $\text{NO}_3^-$  concentrations in all volcanic deposits from this  
111 study, comparable to  $\text{SO}_4^{2-}$  concentrations in most samples, including fully welded ignimbrites.  
112 Nitrate in volcanic deposits has hardly been reported in previous studies and yet several features  
113 indicate that most of this  $\text{NO}_3^-$  was formed during the volcanic eruptions.

114 First,  $\text{NO}_3^-$ ,  $\text{SO}_4^{2-}$  and  $\text{Cl}^-$  contents are found to be well correlated in all samples (Fig.2), which  
115 suggests they share a common origin. As large volcanic eruptions directly release large amounts  
116 of sulphur and halogens in the atmosphere, their origin in volcanic deposits is overwhelmingly  
117 volcanic. Second, the two types of analysed volcanic deposits (ignimbrite and fallout) show  
118 similar elemental compositions (Fig. 2), indicating that the incorporation of external  $\text{NO}_3^-$  by long-  
119 term atmospheric deposition and accumulation since the eruptions (few millions of years) cannot  
120 be dominant in most samples. Indeed, such a post-depositional process should affect more fallout  
121 deposits than ignimbrites because ignimbrites are generally less porous and much denser than  
122 fallout deposits, particularly some of the fully welded ignimbrites units which become quasi-  
123 impermeable by welding typically a decade after deposition (14). Therefore, if a contribution of  
124 long-term atmospheric deposition followed by fluid percolation and accumulation over long  
125 timescales (millions of years) could not be ruled out for the most porous volcanic deposits, this  
126 mechanism cannot explain large amounts of nitrate found within the fully welded ignimbrites.  
127 Finally, in these regions, volcanic deposits are covered by other deposits, which reduce their  
128 exposure time to the atmosphere and its nitrate deposition overtime. The effect of long-term  
129 atmospheric deposition is expected to be much less effective in the youngest deposits from a  
130 non-arid environment (Ischia samples). Nevertheless, large amounts of nitrates (up to 450ppm)  
131 are also measured in these young volcanic deposits. The absence of a positive correlation  
132 between the age of the deposit and its concentration in nitrate suggests that the nitrate found in

133 volcanic deposits is not related to a slow mechanism operating on very long timescales after the  
134 deposit emplacement but rather to the volcanic eruption itself. Third, Anatolian samples collected  
135 in different stratigraphic layers in a fallout deposit of a single volcanic event show a quasi-  
136 systematic increase in  $\text{NO}_3^-$ ,  $\text{SO}_4^{2-}$  and  $\text{Cl}^-$  concentrations from the top to the base of the deposit.  
137 Note that a similar pattern is also observed in the fallout deposits from the younger Tischiello  
138 eruption (Ischia). Fluid circulation (rainwater percolating through the deposit) can affect the  
139 repartition of anions in the deposits, but at least two observations do not support the prevailing  
140 role of this process in our volcanic deposits. i) the concentration enrichments of the salts ( $\text{NO}_3^-$ ,  
141  $\text{SO}_4^{2-}$  and  $\text{Cl}^-$ ) from the top to the base of the deposits is higher for chlorine, than for nitrate and  
142 then sulphate which is not in full accordance with their relative solubilities and hence mobilities in  
143 the deposits. ii) The concentration profiles are not found to be dependent on the deposit thickness  
144 (from 0.7 m to  $\approx 10$  m; (Figure S1)), contrary to what would be expected, i.e. the thinnest deposits  
145 being more washed out than the thickest. Such vertical zoning, also typically observed in major  
146 and trace elements concentrations in volcanic clasts is explained by a stratified magma reservoir  
147 (15). The most volatile-enriched part of the reservoir that is discharged in the early stage of the  
148 eruption is deposited first and forms to the base of the volcanic fallout deposit. The vertical zoning  
149 for nitrate may have been accentuated by the general decreasing intensity of the volcanic  
150 explosivity as an eruption goes on, and hence decreasing volcanic lightning and associated fixed  
151 N generation, as discussed below.

152

153 ***Nitrate generated by  $\text{NO}_x$  oxidation via  $\text{O}_3$ :*** We use the multi-isotopic composition ( $\delta^{15}\text{N}$ ,  $\delta^{18}\text{O}$   
154 and  $\Delta^{17}\text{O}$ ) of nitrates extracted from the volcanic deposits by sample leaching to characterise  
155 their origins. Isotopic composition of compounds provides insights into emission sources and  
156 formation processes. In particular, triple oxygen isotope ( $\delta^{18}\text{O}$ ,  $\Delta^{17}\text{O}$ ) measurements allow us to  
157 trace back the oxidation pathways leading to the formation of  $\text{NO}_3^-$  or sulphate ( $\text{SO}_4^{2-}$ ) (16). The  
158 measurements show that the nitrates in the majority of the samples exhibit large positive oxygen  
159 mass-independent isotopic signature ( $\Delta^{17}\text{O} > 0 \text{‰}$ ) (Fig. 3). Such isotopic anomaly can only be  
160 inherited from the atmospheric ozone molecule ( $\text{O}_3$ ), revealing the atmospheric origin of nitrate  
161 (17). Indeed, NO formed or emitted in the atmosphere acquires an oxygen mass-independent  
162 isotopic anomaly during its oxidation to  $\text{NO}_2$  via its reaction with  $\text{O}_3$ , the  $\Delta^{17}\text{O} > 0 \text{‰}$  source  
163 molecule; then  $\text{NO}_2$  is partly oxidized to nitrate via again reactions involving  $\text{O}_3$  (17). In contrast,  
164 biological nitrates systematically exhibit a  $\Delta^{17}\text{O} \approx 0 \text{‰}$  (18). In the same way, significant positive  
165 ( $> 2 \text{‰}$ )  $\Delta^{17}\text{O}$  signatures in volcanic  $\text{SO}_4^{2-}$  can only be present if S-bearing gases are oxidized by  
166 atmospheric  $\text{O}_3$  or certain  $\text{O}_3$ -derived oxidants(19).  $\Delta^{17}\text{O}_{(\text{NO}_3^-)}$  and  $\Delta^{17}\text{O}_{(\text{SO}_4^{2-})}$  are found to be

167 somewhat correlated (Figure S2) with a slope of  $\sim 2.9$ , which is consistent with atmospheric  
168 oxidation of precursor gases (e.g. NO, SO<sub>2</sub>) involving ozone.

169 About 83 % of the samples display  $\Delta^{17}\text{O} > 0 \text{ ‰}$  and lines up between two endmembers  
170 EM1 and EM2 in a  $\Delta^{17}\text{O} - \delta^{18}\text{O}$  diagram (Fig. 3). EM1-NO<sub>3</sub><sup>-</sup> results necessarily from the NO<sub>x</sub>  
171 oxidation by O<sub>3</sub> ( $\Delta^{17}\text{O} \approx 35 \text{ ‰}$  (20)). EM2-NO<sub>3</sub><sup>-</sup> is characterised by  $\Delta^{17}\text{O}$  close to zero and small  
172 positive  $\delta^{18}\text{O}$  values, which are rather indicative of NO<sub>3</sub><sup>-</sup> from NO<sub>x</sub> oxidation by oxidants carrying  
173 a  $\Delta^{17}\text{O} = 0 \text{ ‰}$  (e.g. tropospheric OH-radicals (21)), though a contribution of biological NO<sub>3</sub><sup>-</sup> cannot  
174 be ruled out. The lining up between EM1 and EM2 reflects the varying contributions of different  
175 pathways to NO<sub>x</sub> oxidation, possibly reflecting the range of emissions and environmental  
176 conditions covered by the various volcanic events considered here. For instance, the conditions  
177 in a PDC (dense cloud moving along the ground level; high temperatures) are drastically different  
178 from the conditions in a Plinian column (volcanic plumes rising, expanding and mixing with the  
179 background atmosphere; ambient temperatures). Even for a single volcanic plume, the  
180 composition evolves rapidly, with oxidation pathways changing between the core and the edge of  
181 the plume depending on atmospheric dispersion and mixing, and the presence of highly effective  
182 ozone-destroying halogens (22). Biologically produced nitrates, represented by the EM3-NO<sub>3</sub>  
183 end-member (Fig. 3, Figure S3 and Supplementary Text), appear to slightly contribute to the total  
184 nitrate content in our samples (17%). On the whole, the multi-isotopic composition of our samples  
185 implies that most of the NO<sub>3</sub><sup>-</sup> in the volcanic deposits originates from NO oxidation in the  
186 atmosphere.

187 The remaining question concerns the sources of NO<sub>x</sub> in the volcanic plumes and PDCs.  
188 N<sub>2</sub> can be released from the magma but only in very low quantities ( $\approx 10^9\text{-}10^{10} \text{ mol.yr}^{-1}$  (23), which  
189 cannot account for the nitrate amount measured in our samples. Gaseous fixed N species (HNO<sub>3</sub>,  
190 NH<sub>3</sub> and NO<sub>x</sub> = NO + NO<sub>2</sub>) have been detected in passive degassing volcanic plumes (not due to  
191 explosive eruptions, (24, 25) but again at very low concentrations, generally at least two orders of  
192 magnitude lower than sulphur concentrations (24). Some of these detections were attributed to  
193 thermal fixation of N<sub>2</sub> above hot lava lakes (26). This mechanism requires a relatively long  
194 exposure of N<sub>2</sub> to lava with high temperatures (>1000°C). During explosive caldera-forming  
195 eruptions, the lava typically displays lower temperatures (800-900°C) and cools down very quickly  
196 in contact with the atmosphere (27, 28). Therefore, it is unlikely that N<sub>2</sub> thermal fixation can  
197 account for the very high NO<sub>3</sub><sup>-</sup> concentration measured in our samples.

198

199 **NO<sub>x</sub> production by volcanic lightning:** The most plausible mechanism able to produce vast  
200 amounts of NO<sub>x</sub> during large explosive eruptions appears to be volcanic lightning (3, 29). Several

201 electrification mechanisms are thought to play a role in VL. This includes ice charging, the  
202 primary mechanism for ordinary storm lightning, particularly effective when a volcanic plume, rich  
203 in water, rises up high into the air (5). Other mechanisms more specific to volcanic eruptions can  
204 also contribute to the electrification of volcanic plumes, notably mechanisms for which the main  
205 carriers of electrical charges are rock/ash particles instead of hydrometeors. Note that the  
206 quantification of electrification mechanisms at play in volcanic plumes, including interactions  
207 between volcanic particles and hydrometeors, remain relatively poor. The potential intensity of  
208 volcanic lightning has been well illustrated by the recent 2022 Hunga Tonga Plinian eruption  
209 where about 400 000 lightning strikes were detected in only 6 hours during the main hydro-  
210 magmatic explosive phase of the eruption (30). Different electrification mechanisms are expected  
211 to dominate depending on the surrounding conditions, composition of the volcanic jet, and  
212 dynamics, typically a rising convective plume versus a pyroclastic flow. For instance, the intensity  
213 of ice charging lightning should largely depend on the plume water content and height whereas  
214 the volcanic particles lightning should depend, among other factors, on the plume ash content.  
215 Although lightning in PDCs is far less studied, the lightning activity is generally more intense in  
216 volcanic plumes because they reach higher altitudes than in PDCs where most of the lightning  
217 occur in the ash cloud/plume above the flow (31).

218 NO produced by lightning is oxidised to NO<sub>2</sub> in a few minutes and NO<sub>x</sub> (NO + NO<sub>2</sub>) is  
219 oxidised to HNO<sub>3</sub> or NO<sub>3</sub><sup>-</sup> in hours/days following different oxidation pathways (32, 33).  
220 Considering the high particle concentrations and water content often found in large volcanic  
221 plumes, heterogeneous chemical pathways for NO<sub>x</sub>-to-nitrate conversion, though uncertain,  
222 should prevail. A large part of the produced nitrate is subsequently adsorbed onto settling  
223 volcanic clasts. Ultimately, the volcanic lightning nitrate, referred as vLNO<sub>3</sub> thereafter, ends up  
224 archived in volcanic deposits over geological times in dry environments (Fig. 4). Overall, our data  
225 show that volcanic lightning during caldera-forming eruptions can be an efficient abiotic N-fixation  
226 process, and that the presence of vLNO<sub>3</sub> in dry volcanic deposits is probably more frequent than  
227 previously thought.

228

229 **Quantification of N-fixation during caldera forming eruptions:** The amounts of vLNO<sub>3</sub>  
230 produced during the very large explosive volcanic eruptions analysed here can be crudely  
231 estimated by considering the density and volume of each volcanic deposit layer and its mean  
232 NO<sub>3</sub><sup>-</sup> concentration. The mean mass of N per single caldera-forming eruption varies strongly from  
233 0.02Tg to 282Tg, with an average of 60Tg over the 9 volcanic events from this study  
234 (Supplementary Table S3). Some of this variability is certainly caused by the high spatial

235 heterogeneity in nitrate deposits and by the varying electrifying plume conditions, notably the  
236 plume water content. Note that one such large explosive eruption can possibly deliver up to about  
237 1 year of biological and anthropogenic global present-day fixed-N production (1) over a limited  
238 area. This range estimated from our data can be compared to theoretical calculations (3) that  
239 derive electrical power generated by volcanic lightning based on the volcanic ash output  
240 assuming that all electrical charges are only carried by ash particles. Since other electrification  
241 mechanisms of volcanic plumes are ignored, in particular the ice driven mechanism, the electric  
242 power available in explosive volcanic eruptions can be considerably underestimated in these  
243 calculations. The NO production by VL was estimated at  $5 \cdot 10^{12}$  g (equivalent to  $1 \cdot 10^{13}$  g of nitrate)  
244 for  $1.3 \cdot 10^{15}$  kg of volcanic ash, which corresponds to a nitrate concentration in ash deposit of  
245 about 10 ppm (10  $\mu$ g of nitrate per gr of volcanic ash). Interestingly, this estimate of 10 ppm falls  
246 in the lower end of our range (1 to 2700 ppm, see supplementary Table S3 for the 9 analysed  
247 eruptive events), which is consistent with this calculation being a conservative estimate, only N  
248 fixation from injected ash is considered.

249

## 250 **Implications**

251

252 The discovery of nitrate in volcanic deposits makes them the first field evidence and geological  
253 archive of N-fixation by volcanic lightning, and this can have important implications. First, volcanic  
254 activity had already been mentioned as a possible source of the Atacama Desert nitrate deposits,  
255 but this possibility has been mostly discounted recently in favour of an atmospheric origin (13,  
256 34). One of the main arguments was that volcanism could not generate nitrates with  $\Delta^{17}\text{O} > 0\text{‰}$ ,  
257 as measured in the Atacama's deposits. Our results indicate that, on the contrary, volcanic  
258 lightning during large explosive eruptions produces  $\nu\text{LNO}_3$  with positive  $\Delta^{17}\text{O}$ . A possible  
259 contribution of the intense Miocene-Quaternary volcanic activity to the Atacama basin nitrates  
260 (34) could be reconsidered. Second, the fact that massive volcanic eruption can fix nitrogen on  
261 that scale has possible implications for life emergence on Earth. In most hypothesis attempting to  
262 explain the emergence and development of life, assimilable N forms are necessary and thus  $\text{N}_2$   
263 must be extensively fixed (35, 36). Ordinary (non-volcanic) lightning has been one of the most  
264 discussed and well-established abiotic N-fixation mechanisms (3, 37, 38). Our findings also hint  
265 at potentially extremely high local contributions of VL from very large subaerial explosive  
266 eruptions, which were already occurring on the early Earth (39, 40). Indeed, nitrates produced by  
267 storm lightning all around the world are spread out on the Earth surface, while volcanic deposits  
268 are formed locally in a very short period of time and, according to our results, can contain large  
269 amounts of fixed N, a prerequisite for the development of life. Obviously, reactive N molecules  
270 and chemistry involved in an oxygen-poor atmosphere on the early Earth would be very different

271 from those occurring in the oxygen-rich atmosphere (36). Nonetheless, in the early Earth  
272 atmosphere (N<sub>2</sub>-CO<sub>2</sub>-rich and O<sub>2</sub>-poor), if expected end-products are more reduced N-  
273 compounds than nitrate (e.g. ammonia) due to the lack of oxygen, it appears that the nitrogen  
274 fixation remains as efficient as in the modern and oxidant atmosphere (N<sub>2</sub>-O<sub>2</sub>-rich) (41).  
275 Heterogeneous reactions occurring in a volcanic plume that is rich in oxides, with magmatic  
276 silicate glass and water in the first place, could provide a more favourable N-fixation environment  
277 than storm (non-volcanic) lightning that occur in the expected relatively anoxic atmosphere. The  
278 potential role of volcanic lightning is not restricted to N-fixation. It might also be relevant to other  
279 energetically costly transformations, which were essential for life emergence, such as the  
280 synthesis of life building blocks (42) or the conversion of mineral phosphorous into biologically  
281 useable forms (43).

282

283

## 284 **Materials and Methods**

285

286 **Samples from this study** were collected from volcanic tephra fallout deposits and large-volume  
287 pyroclastic density current (PDC) deposits, also called ignimbrites, of up to 550km<sup>3</sup>  
288 (Supplementary Table 3). They are collected in arid to semi-arid environments in Central Turkey  
289 (CAVP for Central Anatolia Volcanic Province) and southern Peru (North of the Andean Central  
290 Volcanic Zone) because leaching and erosion processes are expected to be minimal in these  
291 climatic conditions. This limits the possibility of post-deposition or re-precipitation by fluid  
292 circulation, typically rainwater percolating through the deposit, as NO<sub>3</sub><sup>-</sup> (as well as Cl<sup>-</sup> and SO<sub>4</sub><sup>2-</sup>)  
293 is soluble. Ignimbrites can undergo welding in the few months to years after the emplacement,  
294 limiting its alteration (e.g. infiltration of meteoric water) on geological timescales. Therefore, the  
295 ignimbrite samples are not expected to have been significantly affected by external fluid  
296 circulation, which could either bring in non-volcanic soluble compounds or leach nitrate out of  
297 volcanic deposits. All the samples are collected in deposits from very large explosive and caldera-  
298 forming eruptions (VEI 7) dating from ≈1Ma to ≈20Ma. Samples from tephra fallouts and  
299 ignimbrites were collected in both Turkey and Peru at different distances (up to ≈50km) from the  
300 inferred volcanic centre. In Turkey, samples mainly consist of tephra fallouts, while Peruvian  
301 samples are mostly ignimbrites. In addition, thick Anatolian tephra fallout deposits are also  
302 sampled at different heights within each layer, i.e. base, middle and top of the layer.

303 Samples from Ischia (Italy) have also been collected, and correspond to the Tischiello (~75kyrs;  
304 VEI of about 3-4) and the Monte Epemeo Green Tuff – MEGT (~55kyrs; VEI of about 5-6)  
305 eruptions. The deposits have not been preserved in an arid environment such as those from  
306 Turkey and Peru, which is useful for comparison. Indeed, in such conditions any post-deposition

307 processes such as long-term atmospheric deposition and accumulation of nitrates (and other  
308 compounds) in the deposit are precluded.

309

310 **Nitrate, sulphate and chlorine concentrations analyses** are conducted at the analytical  
311 platform Alipp6 (ISTeP-Sorbonne University, Paris) after crushing and leaching the samples (55  
312 and 36 samples for Turkey and Peru, respectively) in deionised water. After filtering the leaching  
313 solutions at 0.45µm, its anionic content is measured using ion chromatography (Dionex ICS  
314 1100, Thermo Scientific) specifically calibrated for sulphate (SO<sub>4</sub><sup>2-</sup>), nitrate (NO<sub>3</sub><sup>-</sup>), and chlorine  
315 (Cl<sup>-</sup>) ions. NO<sub>3</sub><sup>-</sup> and SO<sub>4</sub><sup>2-</sup> from the leachates are separated via the RMSEP (44), and their multi-  
316 isotopic analyses are carried out (on 27 and 8 samples for Turkey and Peru, respectively) (44,  
317 45).

318

319 **Oxygen multi-isotopic analyses on sulphate** were performed at the IPGP Stable Isotope  
320 Laboratory (Paris, France). O-multi-isotopic analyses were performed using the laser fluorination  
321 method (44) on 2-4mg of barite (BaSO<sub>4</sub>). After fluorination of the sample under 40 Torr of BrF<sub>5</sub>,  
322 extracted O<sub>2</sub> is purified through a series of liquid nitrogen and slush traps and collected on a  
323 molecular sieve. The purified O<sub>2</sub> is then injected into a Delta-V Isotope Ratio Mass Spectrometer  
324 (Thermo Fischer Scientific) run in dual inlet to monitor the m/z: 32, 33 and 34, used to determine  
325 the δ<sup>17</sup>O and δ<sup>18</sup>O. The Δ<sup>17</sup>O is then calculated according to the following expression (46): Δ<sup>17</sup>O=  
326 δ<sup>17</sup>O – [(δ<sup>18</sup>O + 1)<sup>0.5305</sup>-1]. While the reproducibility on the international standard NBS127 is ±0.4‰  
327 and ±0.04‰ for δ<sup>18</sup>O and Δ<sup>17</sup>O, the overall reproducibility of the method (leaching, filtration,  
328 RMSEP, O-extraction line and mass spectrometer) is ±1‰ and ±0.1‰ for δ<sup>18</sup>O and Δ<sup>17</sup>O.

329

330 **The multi-isotope analyses on nitrate** (δ<sup>18</sup>O, δ<sup>17</sup>O and δ<sup>15</sup>N) were performed at the  
331 Environmental Geosciences Institute (IGE; Grenoble, France). We used the bacterial denitrifier  
332 method (16) with *Pseudomonas aureofaciens* bacteria. These bacteria transform nitrate from  
333 samples into N<sub>2</sub>O through different reactions. The produced N<sub>2</sub>O is thus loaded into the  
334 purification line. It passes through a series of liquid nitrogen traps and columns, before being  
335 heated up at 900°C, which leads to its decomposition into N<sub>2</sub> and O<sub>2</sub> (47). These two compounds  
336 are separated through a chromatographic column before being injected into a MAT253 Isotope  
337 Ratio Mass Spectrometer. Its configuration allows the successive measurement of oxygen and  
338 nitrogen isotopes. The uncertainties associated are ±1.5‰, ±0.4‰ and ±0.2‰ for δ<sup>18</sup>O, Δ<sup>17</sup>O and  
339 δ<sup>15</sup>N respectively.

340

341

342

343 **Acknowledgments**

344

345 We are very grateful to Sorbonne University for its financial support through the “Emergence” as  
346 well as the “Multi-disciplinary PhD Project” grants (grant n°S18JR311242 and the grant for the A.  
347 Aroskay PhD). This research has also been supported by the Agence Nationale de la Recherche  
348 (PALEOx project, grant no. ANR-16-CE31-0010), IDEX project (grant no. ANR-15-IDEX-02),  
349 Labex OSUG@2020 project (Investissements d’avenir, grant no. ANR10 LABX56). We also  
350 thank E. Gautier and N. Caillon for the O and N multi-isotopic analyses on nitrates, as well as P.  
351 Cartigny for its help for the sulphate isotopic measurements. We are grateful to J-C Thouret for  
352 sharing his knowledge about the Peruvian ignimbrites. We are also grateful to Ilenia Arienzo  
353 (INGV Napoli), Sandro de Vita (INGV Napoli) and Richard Brown (Durham University) for  
354 providing us the Ischia samples. The discussion with H. Martin on the early Earth were deeply  
355 appreciated. Finally, this manuscript was improved by the constructive comments from two  
356 anonymous reviewers.

357

358 **Figure legends**

359

360 **Fig. 1. Intense volcanic lightning during the Calbuco eruption (VEI 4), Chile, in 2015.**  
361 Photography by Francisco Negroni using a few seconds exposure time  
362 (<https://www.francisconegroni.com>).

363

364 **Fig. 2. Correlation between  $\text{NO}_3^-$ ,  $\text{SO}_4^{2-}$  and  $\text{Cl}^-$  measurements in Anatolian (diamonds),**  
365 **Peruvian (circles) and Italian (squares) samples.** Filled and empty symbols represent tephra  
366 fallout and ignimbrite samples, respectively. Dash lines and regular lines represent the correlation  
367 line for Peruvian (n=36) and Anatolian (n=55) samples, respectively. Correlation coefficients are  
368 indicated for each plot.

369

370 **Fig. 3.  $\Delta^{17}\text{O}$  vs.  $\delta^{18}\text{O}$  in Anatolian (n=27), Peruvian (n=8) and Italian (n=3) volcanic deposits.**  
371 Analytical uncertainties (in  $2\sigma$ ) are 1.5 and 0.4 for  $\delta^{18}\text{O}$  and  $\Delta^{17}\text{O}$ , respectively. EM1 represents  
372 nitrates generated by  $\text{NO}_x$  oxidation via ozone. EM2 represents atmospheric nitrates formed via  
373 the oxidation of  $\text{NO}_x$  by an atmospheric oxidant with  $\Delta^{17}\text{O}=0\text{‰}$  and possibly biological nitrates.  
374 Blue symbols, which are well correlated in the  $\Delta^{17}\text{O}$  vs.  $\delta^{18}\text{O}$  plot, correspond to nitrates with co-  
375 varying  $\Delta^{17}\text{O}$ - $\delta^{18}\text{O}$  isotopic compositions, they line up along with the EM1-EM2 mixing line (dotted  
376 line). EM3- $\text{NO}_3^-$  (light brown) represent biological nitrates.

377

378 **Figure 4 | The different formation pathways of nitrates collected in our volcanic deposits**  
379 **are summarised in this schema.** Lightning occurring in volcanic plumes and in PDCs produces  
380 NO<sub>x</sub> from atmospheric N<sub>2</sub>. They are then oxidized into nitrates by O<sub>3</sub> leading to EM1-NO<sub>3</sub><sup>-</sup> with a  
381  $\Delta^{17}\text{O} \sim 30\text{--}40\text{‰}$ . Some NO<sub>x</sub> can be oxidized by compounds such as OH radicals in the  
382 troposphere leading to EM2-NO<sub>3</sub><sup>-</sup> with a  $\Delta^{17}\text{O} = 0\text{‰}$ . It cannot be ruled out that biological nitrates  
383 that have a  $\Delta^{17}\text{O} = 0\text{‰}$  also contribute to EM2-NO<sub>3</sub><sup>-</sup>. In both cases, nitrates coming from EM1 +  
384 EM2-NO<sub>3</sub><sup>-</sup> show a  $\Delta^{17}\text{O} \geq 0\text{‰}$  whose value depends on the relative proportions of the nitrate  
385 sources. Biological nitrates resulting from bacterial nitrification with  $\Delta^{17}\text{O}=0\text{‰}$  (EM3-NO<sub>3</sub><sup>-</sup> and  
386 possibly part of EM2-NO<sub>3</sub><sup>-</sup>) are identified in few volcanic deposits.

387

388

### 389 **References**

390

- 391 1. P. Ciais, C. Sabine, “Carbon and Other Biogeochemical Cycles” (2013)  
392 <https://doi.org/10.1017/CBO9781107415324.015>.
- 393 2. D. E. Canfield, A. N. Glazer, P. G. Falkowski, The evolution and future of earth’s nitrogen  
394 cycle. *Science (80-. )*. **330**, 192–196 (2010).
- 395 3. R. Navarro-Gonzalez, M. J. Molina, L. T. Molina, Nitrogen fixation by volcanic lightning in  
396 the early Earth. *Geophys. Res. Lett.* **25**, 3123–3126 (1998).
- 397 4. A. Segura, R. Navarro-González, Nitrogen fixation on early Mars by volcanic lightning and  
398 other sources. *Geophys. Res. Lett.* **32**, 1–4 (2005).
- 399 5. C. Cimarelli, K. Genareau, A review of volcanic electrification of the atmosphere and  
400 volcanic lightning. *J. Volcanol. Geotherm. Res.* **422**, 107449 (2022).
- 401 6. S. A. Behnke, *et al.*, Discriminating Types of Volcanic Electrical Activity : Toward an  
402 Eruption Detection Algorithm. 1–9 (2022).
- 403 7. C. Cimarelli, S. Behnke, K. Genareau, J. Méndez, H. Alexa, Volcanic electrification :  
404 recent advances and future perspectives. *Bull. Volcanol.* **84**, 1–10 (2022).
- 405 8. R. S. Martin, T. A. Mather, D. M. Pyle, Volcanic emissions and the early Earth  
406 atmosphere. *geochemica Cosmochem. acta* **71**, 3673–3685 (2007).
- 407 9. R. Navarro-Gonzalez, C. P. McKay, D. Nna Mvondo, A possible nitrogen crisis for  
408 Archaean life due to reduced nitrogen fixation by lightning. *Nature* **412**, 61–64 (2001).

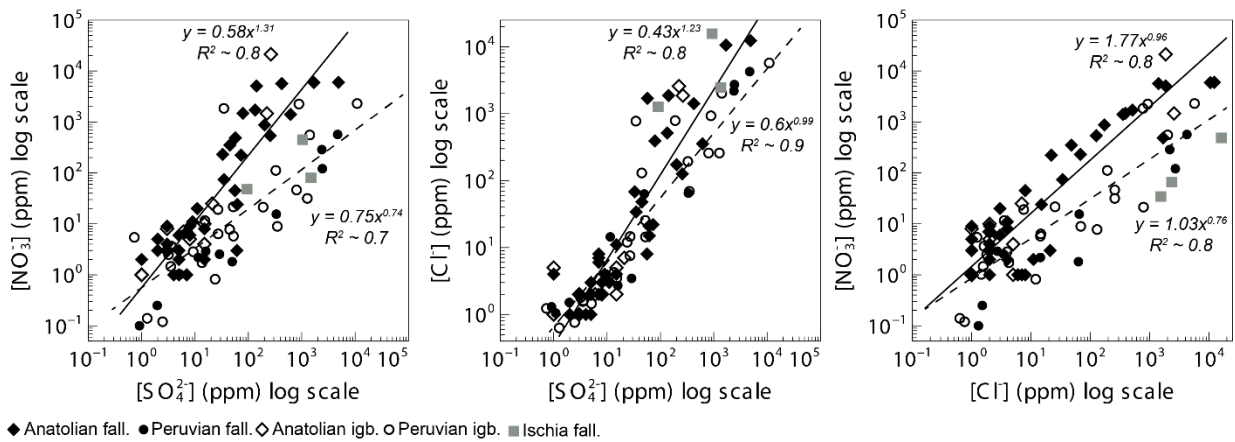
- 409 10. J.-L. Le Pennec, *et al.*, Neogene ignimbrites of the Nevsehir plateau (central Turkey)"  
410 stratigraphy, distribution and source constraints. *J. Volcanol. Geotherm. Res.* **63**, 59–87  
411 (1994).
- 412 11. P. Paquereau, J. Thouret, G. Wörner, M. Fornari, Neogene and Quaternary ignimbrites in  
413 the area of Arequipa , Southern Peru : Stratigraphical and petrological correlations. *J.*  
414 *Volcanol. Geotherm. Res.* **154**, 251–275 (2006).
- 415 12. R. J. Brown, G. Orsi, S. De Vita, New insights into Late Pleistocene explosive volcanic  
416 activity and caldera formation on Ischia ( southern Italy ). *Bull. Volcanol.*, 583–603 (2008).
- 417 13. G. Michalski, J. K. Böhlke, M. Thiemens, Long term atmospheric deposition as the source  
418 of nitrate and other salts in the Atacama Desert, Chile: New evidence from mass-  
419 independent oxygen isotopic compositions. *Geochim. Cosmochim. Acta* **68**, 4023–4038  
420 (2004).
- 421 14. F. B. Wadsworth, *et al.*, Universal scaling of fluid permeability during volcanic welding and  
422 sediment diagenesis. *Geology* **44**, 219–222 (2016).
- 423 15. G. C. Kennedy, Some Aspects of the Role of Water In Rock Melts. *Geol. Soc. Am.*, 489–  
424 504 (1955).
- 425 16. S. Morin, *et al.*, Signature of Arctic surface ozone depletion events in the isotope anomaly  
426 (  $^{17}\text{O}$  ) of atmospheric nitrate. *Atmos. Chem. Phys.*, 1451–1469 (2007).
- 427 17. G. Michalski, Z. Scott, M. Kabling, M. H. Thiemens, First measurements and modeling of  
428  $\Delta^{17}\text{O}$  in atmospheric nitrate. *Geophys. Res. Lett.* **30**, 3–6 (2003).
- 429 18. C. Kendall, E. M. Elliott, S. D. Wankel, *Tracing anthropogenic inputs of nitrogen to*  
430 *ecosystems* (2007).
- 431 19. E. Martin, Volcanic Plume Impact on the Atmosphere and Climate : O- and S-Isotope  
432 Insight into Sulfate Aerosol Formation. *geosciences*, 1–23 (2018).
- 433 20. W. C. Vicars, J. Savarino, Quantitative constraints on the  $^{17}\text{O}$ -excess ( $\delta^{17}\text{O}$ ) signature of  
434 surface ozone: Ambient measurements from  $50^\circ\text{N}$  to  $50^\circ\text{S}$  using the nitrite-coated filter  
435 technique. *Geochim. Cosmochim. Acta* **135**, 270–287 (2014).
- 436 21. J. Savarino, C. C. W. Lee, M. H. Thiemens, Laboratory oxygen isotopic study of sulfur (IV)  
437 oxidation: Origin of the mass-independent oxygen isotopic anomaly in atmospheric  
438 sulfates and sulfate mineral deposits on Earth. *J. Geophys. Res.* **105** (2000).

- 439 22. L. Surl, T. Roberts, S. Bekki, Observation and modelling of ozone-destructive halogen  
440 chemistry in a passively degassing volcanic plume. *Atmos. Chem. Phys.* **21**, 12413–  
441 12441 (2021).
- 442 23. T. P. Fischer, *et al.*, Subduction and recycling of nitrogen along the Central American  
443 margin. *Science (80-. )*. **297**, 1154–1157 (2002).
- 444 24. R. S. Martin, J. C. Wheeler, E. Ilyinskaya, C. F. Braban, C. Oppenheimer, The uptake of  
445 halogen ( HF , HCl , HBr and HI ) and nitric ( HNO<sub>3</sub> ) acids into acidic sulphate particles  
446 in quiescent volcanic plumes. *Chem. Geol.* **296–297**, 19–25 (2012).
- 447 25. T. A. Mather, *et al.*, Nitric acid from volcanoes. *Earth Planet. Sci. Lett.* **218**, 17–30 (2004).
- 448 26. T. A. Mather, D. M. Pyle, A. G. Allen, Volcanic source for fixed nitrogen in the early Earth '  
449 s atmosphere. *Geology*, 905–908 (2004).
- 450 27. Y. Sawada, Y. Sampei, M. Hyodo, T. Yagami, M. Fukue, Estimation of emplacement  
451 temperature of pyroclastic flows using H/C ratios of carbonized wood. *J. Volcanol.*  
452 *Geotherm. Res.* **104**, 1–20 (2000).
- 453 28. A. C. Scott, R. S. J. Sparks, I. D. Bull, H. Knicker, R. P. Evershed, Temperature proxy  
454 data and their significance for the understanding of pyroclastic density currents. *Geology*  
455 **36**, 143–146 (2008).
- 456 29. A. R. Bandy, P. J. Maroulis, L. A. Wilner, A. L. Torres, Estimates of the fluxes of NO, SO<sub>2</sub>,  
457 H<sub>2</sub>S, CS<sub>2</sub>, and OCS from Mt. St. Helens deduced from in situ plume concentration  
458 measurements. *Geophys. Res. Lett.* **9**, 1097–1100 (1982).
- 459 30. M. Sharma, S. Scarr, Tonga eruption: the perfect storm. *graphics.reuters.com* (2022).
- 460 31. T. Miura, T. Koyaguchi, Y. Tanaka, Atmospheric electric potential gradient measurements  
461 of ash clouds generated by pyroclastic flows at Unzen volcano, Japan. *Geophys. Res.*  
462 *Lett.* **23**, 1789–1792 (1996).
- 463 32. S. Morin, *et al.*, Tracing the origin and fate of NO<sub>x</sub> in the Arctic Atmosphere using stable  
464 isotopes in nitrate. *Science (80-. )*. **322**, 730–732 (2013).
- 465 33. U. Schumann, H. Huntrieser, The global lightning-induced nitrogen oxides source. *Atmos.*  
466 *Chem. Phys.* **7**, 3823–3907 (2007).
- 467 34. J. Oyarzun, R. Oyarzun, Massive Volcanism in the Altiplano-Puna Volcanic Plateau and

- 468 Formation of the Huge Atacama Desert Nitrate Deposits: A Case for Thermal and Electric  
469 Fixation of Atmospheric Nitrogen. *Int. Geol. Rev.* **49**, 962–968 (2008).
- 470 35. N. Kitadai, S. Maruyama, Origins of building blocks of life: A review. *Geosci. Front.* **9**,  
471 1117–1153 (2018).
- 472 36. Y. L. Yung, M. B. McElroy, Fixation of nitrogen in the prebiotic atmosphere. *Science* (80-  
473 ). **203**, 1002–1004 (1979).
- 474 37. R. D. Hill, An efficient lightning energy source on the early Earth. *Orig. Life Evol. Biosph.*,  
475 277–285 (1992).
- 476 38. H. Huntrieser, *et al.*, Lightning activity in Brazilian thunderstorms during TROCCINOX:  
477 Implications for NO<sub>x</sub> production. *Atmos. Chem. Phys.* **8**, 921–953 (2008).
- 478 39. W. U. Mueller, R. C. Thurston, *Chapter 4 Precambrian volcanism: An independent*  
479 *variable through time* (Elsevier Masson SAS, 2004).
- 480 40. J. L. Bada, Volcanic Island lightning prebiotic chemistry and the origin of life in the early  
481 Hadean eon. *Nat. Commun.* **14**, 2011 (2023).
- 482 41. P. Barth, *et al.*, Isotopic constraints on lightning as a source of fixed nitrogen in Earth's  
483 early biosphere. *Nat. Geosci.* **16** (2023).
- 484 42. M. Ferus, *et al.*, High Energy Radical Chemistry Formation of HCN-rich Atmospheres on  
485 early Earth. *Sci. Rep.* **7**, 1–9 (2017).
- 486 43. B. L. Hess, S. Piazzolo, J. Harvey, Lightning strikes as a major facilitator of prebiotic  
487 phosphorus reduction on early Earth. *Nat. Commun.* **12**, 1–8 (2021).
- 488 44. H. Bao, M. H. Thiemens, Generation of O<sub>2</sub> from BaSO<sub>4</sub> Using a CO<sub>2</sub>-Laser  
489 Fluorination System for Simultaneous Analysis of δ<sup>18</sup>O and δ<sup>17</sup>O. *Anal. Chem.* **72**,  
490 4029–4032 (2000).
- 491 45. H. Bao, X. Cao, J. A. Hayles, Triple Oxygen Isotopes: Fundamental Relationships and  
492 Applications. *Annu. Rev. Earth Planet. Sci.* **44**, 463–492 (2016).
- 493 46. S. Morin, "Analyse de la composition isotopique de l'ion nitrate dans la basse  
494 atmosphère polaire et marine." (2008).
- 495 47. S. S. Cliff, M. H. Thiemens, High-Precision Isotopic Determination of the <sup>18</sup>O/<sup>16</sup>O and  
496 <sup>17</sup>O/<sup>16</sup>O ratios in nitrous oxide. *Anal. Chem.*, 2791–2793 (1994).



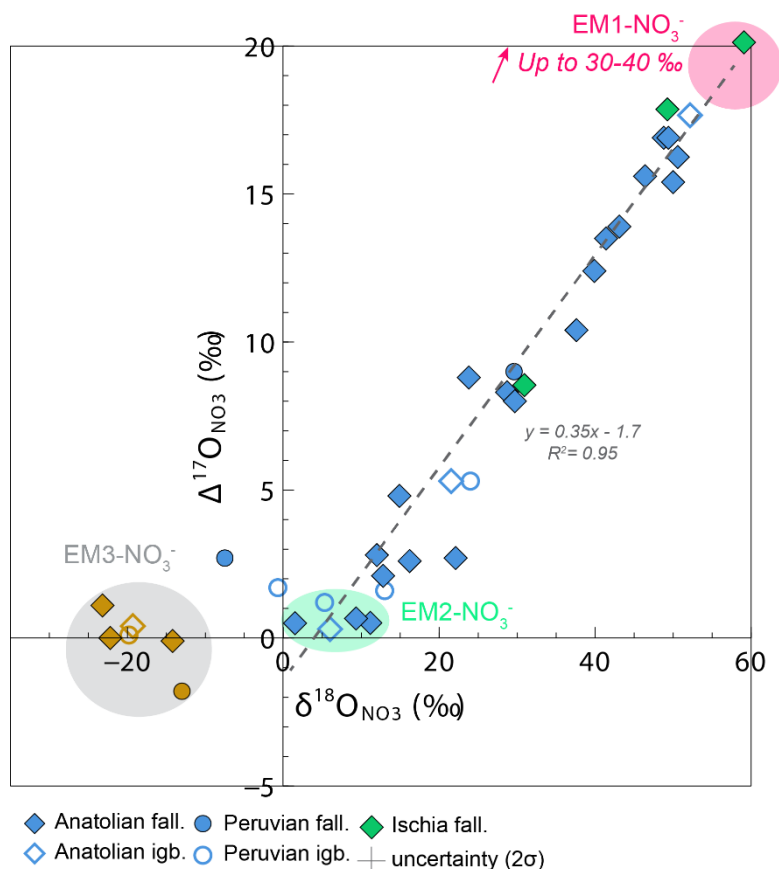
500 **Fig. 1. Intense volcanic lightning during the Calbuco eruption (VEI 4), Chile, in 2015.**  
 501 Photography by Francisco Negroni using a few seconds exposure time  
 502 (<https://www.francisconegroni.com>).



506 **Fig. 2. Correlation between  $\text{NO}_3^-$ ,  $\text{SO}_4^{2-}$  and  $\text{Cl}^-$  measurements in Anatolian (diamonds),**  
 507 **Peruvian (circles) and Italian (squares) samples. Filled and empty symbols represent tephra**

508 fallout and ignimbrite samples, respectively. Dash lines and regular lines represent the correlation  
 509 line for Peruvian (n=36) and Anatolian (n=55) samples, respectively. Correlation coefficients are  
 510 indicated for each plot.

511



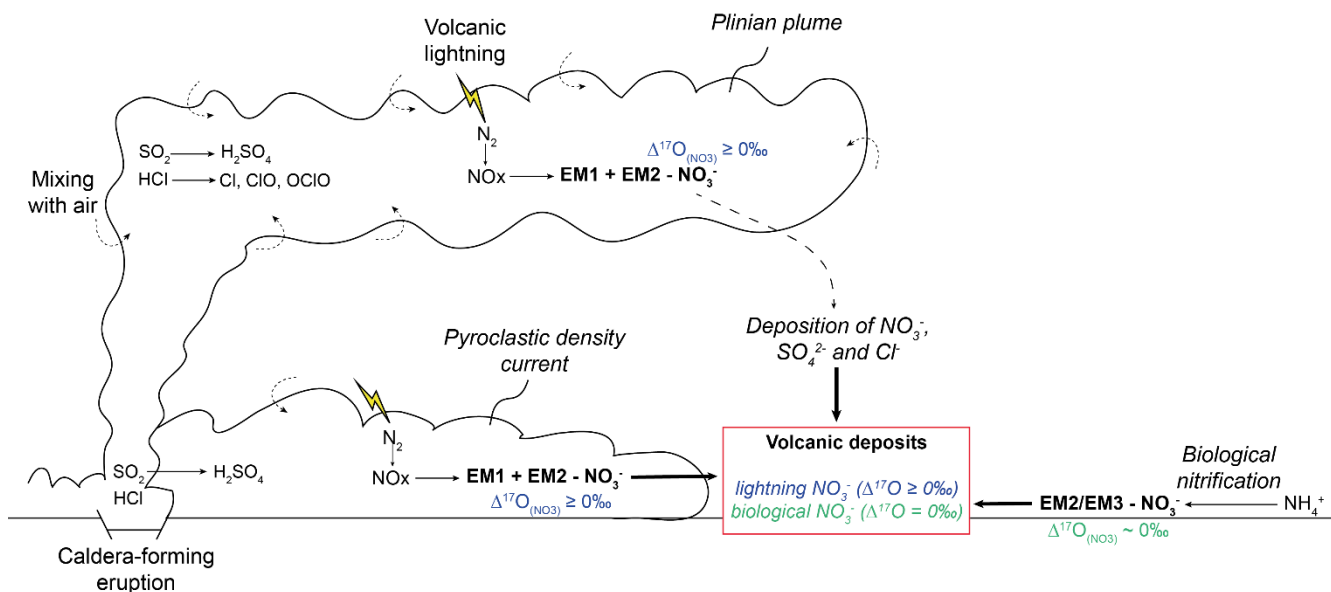
512

513

514 **Fig. 3.  $\Delta^{17}\text{O}$  vs.  $\delta^{18}\text{O}$  in Anatolian (n=27), Peruvian (n=8) and Italian (n=3) volcanic deposits.**

515 Analytical uncertainties (in  $2\sigma$ ) are 1.5 and 0.4 for  $\delta^{18}\text{O}$  and  $\Delta^{17}\text{O}$ , respectively. EM1 represents  
 516 nitrates generated by  $\text{NO}_x$  oxidation via ozone. EM2 represents atmospheric nitrates formed via  
 517 the oxidation of  $\text{NO}_x$  by an atmospheric oxidant with  $\Delta^{17}\text{O}=0\text{‰}$  and possibly biological nitrates.  
 518 Blue symbols, which are well correlated in the  $\Delta^{17}\text{O}$  vs.  $\delta^{18}\text{O}$  plot, correspond to nitrates with co-  
 519 varying  $\Delta^{17}\text{O}$ - $\delta^{18}\text{O}$  isotopic compositions, they line up along with the EM1-EM2 mixing line (dotted  
 520 line). EM3- $\text{NO}_3^-$  (light brown) represent biological nitrates.

521



522

523 **Figure 4 | The different formation pathways of nitrates collected in our volcanic deposits**

524 **are summarised in this schema.** Lightning occurring in volcanic plumes and in PDCs produces

525 NO<sub>x</sub> from atmospheric N<sub>2</sub>. They are then oxidized into nitrates by O<sub>3</sub> leading to EM1-NO<sub>3</sub><sup>-</sup> with a

526 Δ<sup>17</sup>O ~30-40‰. Some NO<sub>x</sub> can be oxidized by compounds such as OH radicals in the

527 troposphere leading to EM2-NO<sub>3</sub><sup>-</sup> with a Δ<sup>17</sup>O = 0‰. It cannot be ruled out that biological nitrates

528 that have a Δ<sup>17</sup>O = 0‰ also contribute to EM2-NO<sub>3</sub><sup>-</sup>. In both cases, nitrates coming from EM1 +

529 EM2-NO<sub>3</sub><sup>-</sup> show a Δ<sup>17</sup>O ≥ 0‰ whose value depends on the relative proportions of the nitrate

530 sources. Biological nitrates resulting from bacterial nitrification with Δ<sup>17</sup>O=0‰ (EM3-NO<sub>3</sub><sup>-</sup> and

531 possibly part of EM2-NO<sub>3</sub><sup>-</sup>) are identified in few volcanic deposits.

532

533